Bull. Chem. Soc. Jpn., 70, 1573—1581 (1997)

Characterization of Dimeric Copper(II) Trichloroacetate Complexes by Electron Spin Resonance, Infrared, and Electronic Reflectance Spectra. Correlation of Spectral Parameters with Molecular Geometry

Yoneichiro Muto,[#] Hiroshi Horie, Tadashi Tokii, Michio Nakashima, Masayuki Koikawa, Omar W. Steward,[†] Shigeru Ohba,[††] Hidehiro Uekusa,[††,##] Steinar Husebye,[†††] Ikuo Suzuki,[††††] and Michinobu Kato*,[†††††, ###]

Department of Chemistry, Faculty of Science and Engineering, Saga University, Saga 840

†Department of Chemistry and Biochemistry, Duquesne University, Pittsburgh, PA 15282, USA

††Department of Chemistry, Faculty of Science and Technology, Keio University, Hiyoshi 3-14-1, Kohoku-ku, Yokohama 223

†††Department of Chemistry, University of Bergen, 5007 Bergen, Norway

††††Department of Electrical and Computer Engineering, Nagoya Institute of Technology, Showa-ku, Nagoya 466

†††††Aichi Prefectural University, Mizuho-ku, Nagoya 467

(Received September 27, 1996)

ESR, IR, and electronic reflectance spectral data are presented for dimeric (trichloroacetato)copper(II) complexes, of which magneto-structural data are available: The larger is the distortion of the coordination geometry from square pyramidal (SP) toward trigonal bipyramidal (TBP), the longer is the Cu···Cu distance in the dimers. The elongation of the Cu···Cu distance is accompanied by a reduction of the zero-field splitting parameter (D), the anisotropic exchange parameter (D^{ex}), and the peak separation of the two peaks in the electronic spectra ($\Delta\overline{\nu}_{max}$). The splitting of the carboxylato stretching frequencies, $\Delta\overline{\nu}$ ($=\overline{\nu}_{asym}-\overline{\nu}_{sym}$), increases with the distortion. Good linear correlations have been observed between the values of these parameters and the Cu···Cu distances. The axial ESR spectra with $g_{/\!/} > g_{\perp}$ and the electronic spectra suggest that the ground state of the Cu atom is essentially $d_{x^2-y^2}$, even in the metal geometry of the greatest distortion toward TBP (the z-axis is along the longest Cu–O bond).

Over the past few decades, extensive magneto-structural studies have been performed concerning dimeric (carboxylato)copper(II) complexes.[1—9] Recently, several nobel results have been reported. For example, (silanecarboxylato)copper(II) complexes show very large singlet–triplet separations, $-2J$=ca. 1000 cm^{-1} ($H=-2JS_1\cdot S_2$), due to the strong σ-electron donating and π-electron back-donating ability of the Si atom, which is directly bonded to the carboxylato bridge.[10,11] An unusually strong antiferromagnetic interaction is also observed in dimeric (benzoylformato)copper(II) complexes ($-2J$=ca. 650 cm^{-1}), and is attributed to an electronic effect of the α-keto group in the bridging carboxylato moiety.[12] These complexes have the typical square pyramidal (SP) coordination geometry. The key factor which affects the $-2J$ value is the electronic structure of the bridging COO^- moiety: the larger is the $2p_x$ orbital population of the carboxylato C atom in the symmetric HOMO of the $RCOO^-$ ion (x is along the C–R bond), the larger is the $-2J$ value of the dimeric (carboxylato)copper(II) complex.[10—12] On the other hand, $[Cu_2(O_2CCPh_3)_4(py)_2]\cdot C_6H_6$ has been shown to have a deformed cage structure, where the coordination geometry is square-pyramidal distorted toward trigonal bipyramidal (SPDTBP).[13] The Cu···Cu distance in the dimer is as long as 3.086 Å, and the $-2J$ value is unusually small (187 cm^{-1}). A similar type of cage deformation has been widely observed in dimeric (trichloroacetato)copper(II) complexes, and there is a clear magneto-structural correlation: The longer is the Cu···Cu distance, the larger is the distortion of the metal geometry from SP toward trigonal bipyramidal (TBP), and the smaller is the $-2J$ value.[14] This fact is explained in terms of a reduced overlaping of the magnetic orbitals.

In this study the ESR, IR, and electronic reflectance spectral data for seventeen (trichloroacetato)copper(II) complexes, whose crystal structures have been reported,[14] were collected in order to see how they change along with a progressive variation of the metal geometry. The entries given

Present address: 13-3, 2-Chome, Mizugae, Saga 840.
Present address: Department of Chemistry, Tokyo Institute of Technology, Ookayama, Meguro-ku, Tokyo 152.
Present address: 5-603, 6, 4-Chome, Kamezaki, Asakita-ku, Hiroshima 739-17.

in Table 1 are tentatively classified into three groups: complexes with the typical SP coordination geometry (Nos. 1—3, $-2J$=229—240 cm^{-1}), complexes showing the greatest distortion from SP toward TBP (Nos. 14—17, $-2J$=79—107 cm^{-1}), and complexes with metal geometries intermediate between these two groups. The cage structures of two representatives are shown in Fig. 1.

Experimental

Syntheses. All of the compounds were prepared by procedures listed elsewhere.[14—19]

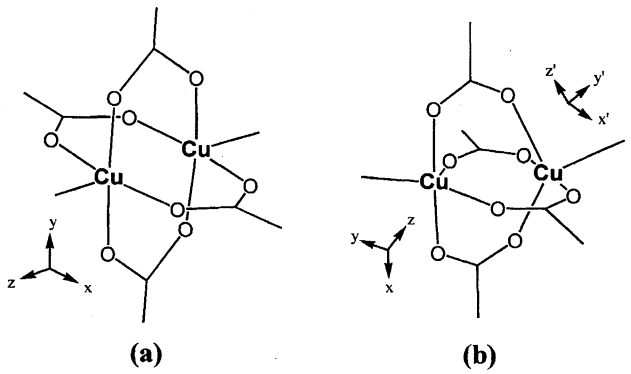

(a) (b)

Fig. 1. Cage structures of two representative complexes of $[Cu_2(O_2CCCl_3)_4(L)_2]\cdot nS$: (a) [(1) SP; $-2J$=240 cm^{-1}] and (b) [(17) SPDTBP; $-2J$=79 cm^{-1}]. The numbers in the parentheses designate the complexes listed in Table 1. The local coordinate axes for Cu atoms are respectively indicated.

Physical Measurements. Polycrystalline powder ESR X-band spectra were recorded with a Jeolco JES-ME 2 Spectrometer at room temperature. The ESR parameters ($g_{/\!/}$, $g_\perp$, and D) were obtained after Boillot et al.[20] They are given in Table 1.[21] The reflectance spectra were obtained on Hitachi 323 and Nihonbunko UV-570DS spectrophotometers. The absorption maxima are listed in Table 3. The IR spectra were recorded on a Perkin–Elmer FT-IR 1760X spectrophotometer (polystyrene standard). The carbon–oxygen stretching frequencies are given in Table 4.

Results and Discussion

Electron Spin Resonance Spectra. The interpretation of the ESR spectral data is based on a method reported by Solomon, et al.[22] for the copper(II) acetate pyrazine complex. The zero-field splitting parameter (D) is given by the sum of two components,[20,22]

$$D = D^{ex} + D^{dip}, \quad (1)$$

where D^{ex} is the component from an anisotropic exchange and D^{dip} is the component from a through-space interaction between the two point magnetic moments centered on the two metal ions,

$$D^{ex} = -1/16(g_{/\!/} - 2)^2 J_{xy,x^2-y^2} + 1/4(g_\perp - 2)^2 J_{xzyz,x^2-y^2}, \quad (2)$$

$$D^{dip} = -(g_{/\!/}{}^2 + 0.5 g_\perp{}^2)\beta^2/r^3, \quad (3)$$

where J_{xy,x^2-y^2} and J_{xzyz,x^2-y^2} are the exchange interactions between an unpaired electron in the $d_{x^2-y^2}$ ground state of a copper ion and a second electron in the d_{xy} and $d_{xz,yz}$ excited states, respectively, of the other copper ion in a dimeric

Table 1. ESR and Related Parameters and the Cu···Cu Distance for $[Cu_2(O_2CCCl_3)_4(L)_2]\cdot nS$[a]

Compound[a]	$g_{/\!/}$	$g_\perp$	g_{av}	D	D^{dip}	D^{ex}	H_0	$-2J$[b]	Cu ··· Cu
				cm^{-1}	cm^{-1}	cm^{-1}	cm^{-1}	cm^{-1}	Å
1	2.379	2.084	2.187	0.369	−0.323	0.692	0.315	240	2.760[c]
2	2.402	2.071	2.187	0.380	−0.317	0.697	0.315	237	2.786[c]
3	2.377	2.083	2.185	0.366	−0.319	0.685	0.315	229	2.769[c]
4	2.388	2.088	2.192	0.364	−0.335	0.699	0.316	224[d]	2.732[d]
5	2.409	2.060	2.183	0.366	−0.335	0.701	0.314	220[c]	2.736[c]
6	2.380	2.074	2.181	0.370	−0.320	0.690	0.315	220[e]	2.766[e]
7	2.381[f]	2.085[f]	2.188[f]	0.359[f]	−0.293	0.652	0.308[f]	195[f]	2.852[f]
8	2.392[g]	2.067[g]	2.181[g]	0.366[g]	−0.319	0.685	0.306	193[g]	2.774[c]
9	2.358	2.096	2.187	0.342	−0.262	0.604	0.314	191	2.951[c]
10	2.337	2.111	2.189	0.315	−0.221	0.536	0.315	141	3.112[c]
11	2.402[g]	2.074[g]	2.189[g]	0.222[g]	−0.238	0.460	0.313	138[g]	3.066[c]
12	2.309[f]	2.107[f]	2.176[f]	0.236[f]	−0.228	0.464	0.314[f]	136[f]	3.062[c]
13	2.286	2.114	2.173	0.249	−0.226	0.475	0.316	131	3.060[c]
14	2.276	2.155	2.196	0.195	−0.201	0.396	0.314	107	3.186[c]
15	2.345	2.088	2.177	0.184	−0.198	0.382	0.309	102	3.226[c]
16	2.294	2.136	2.191	0.181	−0.197	0.378	0.299	95	3.216[c]
17	2.332	2.110	2.186	0.173	−0.192	0.365	0.314	79	3.261[c]

a) Compounds are designated by L, monodentate non-carboxylato ligand, S, solvent molecule, and n, number of solvent molecules: 1: L=2-F-benzothiazol, nS=none; 2: L=4,7-Cl_2-quinoline, nS=none; 3: L=4-CN-py, nS=none; 4: L=PhCN, nS=none; 5: L=1/2Caffeine, nS=2Toluene; 6: L=2-Cl-py, nS=none; 7: L=Caffeine(1), nS=2Benzene;[c] 8: L=3-Cl-py, nS=none; 9: L=2,5-Cl_2-py, nS=none; 10: L=2,5-Cl_2-py, nS=Benzene; 11: L=3-CN-py, nS=none; 12: L=Caffeine(3), nS=none;[c] 13: L=2-Cl-5-NO_2-py, nS=none; 14: L=3,4-Me_2-py, nS=none; 15: L=2,5-Me_2-py, nS=Toluene; 16: L=2,3-Me_2-py, nS=Toluene; 17: L=2-Et-py, nS=none. b) $-2J$, singlet–triplet separation (see Ref. 9); the data in this column are from Refs. 9 and 19 unless otherwise indicated. c) Ref. 14. d) Ref. 15. e) Ref. 18. f) Ref. 17. g) Ref. 16.

copper(II) system. In Eq. 3, r is the Cu···Cu distance. The values of D^{dip} in Table 1 were calculated by Eq. 3 using the values of $g_{//}$, $g_{\perp}$, and r in references.[14] The values of D^{ex} given in Table 1 were obtained by substituting the values of D and D^{dip} into Eq. 1.

The ESR spectral features of a wide range in terms of D from 0.17 to 0.38 cm^{-1} are quite similar to those of the calculated ESR spectra by Pilbrow et al.[23—25] The ESR spectra of some selected complexes are given in Fig. 2. Linear-regression analyses were carried out on the ESR data; the results are given in Table 2. A good linear correlation is observed between the Cu···Cu distances and D^{dip} (see Fig. 3). In our previous study of (trichloroacetato)copper(II) (TCAC) complexes, a good linear correlation with a negative slope was observed for $-2J$ vs. Cu···Cu (Table 2).[14] In the present study, a similar linear correlation for D vs. Cu···Cu is reported, as shown in Fig. 4. Therefore, there should exist a good linear correlation with a positive slope between D and $-2J$. It is remarkable that plots based on ESR data for the complexes are distributed in two separate regions: an SP region (Nos. 1—8) and an SPDTBP region (Nos. 9—17). Such linear correlations as $-2J$ vs. Cu···Cu, D vs. Cu···Cu, and D vs. $-2J$ would be expected based on our previous study on $[Cu_2(O_2CCPh_3)_4(py)_2]\cdot C_6H_6$, which has an unusual SPDTBP metal geometry, to lead to a small $-2J$ value (187 cm^{-1}), a small D value (0.198 cm^{-1}), and a long Cu···Cu distance (3.086 Å).[13] For many (carboxylato)copper(II) complexes with SP metal geometry, the relationship $D>H_0$ has been observed.[23,26,27] However, Steward et al. observed the relationship $D<H_0$ for the complex, $[Cu_2(O_2CCPh_3)_4(py)_2]\cdot C_6H_6$.[13] On the graph of D vs. Cu···Cu in Fig. 4, the complexes distribute distinctively over the two regions, SP ($D>H_0$) and SPDTBP ($D<H_0$). Therefore, at least for dimeric TCAC, we can use the relations $D>H_0$ and $D<H_0$ as an empirical criterion for distinguishing the metal geometry of SP from that of SPDTBP.[9,13,17] It is noteworthy that the linearity of D^{ex} vs. Cu···Cu (Fig. 5) is much better than that of D vs. Cu···Cu. In either diagram, complexes 1—3, which show the typical SP geometry, and 14—17, which show the greatest distortion toward the TBP geometry so far studied, both distribute in a narrow area, indicating that the value of D or D^{ex} reflects the structural characteristics. However, a linear correlation with a positive slope between D and $-2J$ is not a general trend for dimeric (carboxylato)copper(II) complexes. As a matter of fact, our recent magnetic and spectral studies on the SP type of complexes, $[Cu_2(O_2CCMe_nPh_{3-n})_4(L)_2]$ (MPAC), have shown that, in this system, there is a correlation with a negative slope between the values of $-2J$ and D.[28] The mechanism by which the relation between $-2J$ and D differs in these two systems, TCAC (SP–SPDTBP) and MPAC (SP), is a matter which needs further study.[29]

The TCAC complexes show axial spectra with $g_{//}>g_{\perp}$, which is used as a criterion for distinguishing a $d_{x^2-y^2}$ from a d_{z^2} ground state.[30—33] There are a few compounds containing non-carboxylato ligands, such as L=3-Cl-py, where the spectrum is so complicated that it is difficult to reach a

Table 2. The Results of the Linear-Regression Analyses of ESR, IR, and Electronic Reflectance Spectral Data for $[Cu_2(O_2CCCl_3)_4(L)_2]\cdot nS$[a]

Linear correlations	a	b	R^2
D^{dip} vs. Cu···Cu	0.280	−1.09	0.989
D vs. Cu···Cu	−0.389	1.45	0.892
D^{ex} vs. Cu···Cu	−0.669	2.54	0.963
D vs. $-2J$	0.00140	0.0586	0.919
$-2J$ vs. Cu···Cu	−274	980	0.950
$\Delta\bar{\nu}_{max}$ vs. Cu···Cu	−6.48	22.6	0.868
$\Delta\bar{\nu}_{max}$ vs. $-2J$(1)[b]	0.0231	−0.486	0.876
$\Delta\bar{\nu}_{max}$ vs. $-2J$(2)[c]	0.0224	−0.158	0.903
$\Delta\bar{\nu}_{max}$ vs. $-2J$(3)[d]	0.0226	−0.299	0.883
$\Delta\bar{\nu}$ vs. Cu···Cu	83.3	86.3	0.892
$\Delta\bar{\nu}$ vs. $-2J$	−0.287	381	0.837
$\bar{\nu}_{asym}$ vs. Cu···Cu	20.7	1630	0.858
$\Delta\bar{\nu}$ vs. Cu–O (longest)	119	82.2	0.849
$\bar{\nu}_{asym}$ vs. Cu–O (longest)	29.0	1630	0.787
Cu–O (longest) vs. Cu···Cu	0.661	0.155	0.935

a) The equation employed for the analyses is $y=ax+b$, where y is one of the ESR, IR, and electronic reflectance spectral parameters, and x is the Cu···Cu distance except for the case mentioned in particular. The evaluation of the analyses is expressed by the coefficient of determination, R^2, which is the square of the correlation coefficient R. $R=S_{xy}/S_xS_y$, where S_{xy} is the covariance of x and y, and S_x and S_y are the standard deviations of the distributions of x and y. b) Analysis for compounds 1—17 in Table 3. c) Analysis for the lower fourteen compounds designated with non-carboxylato ligand L in Table 3. d) Analysis for the all thirty-one compounds in Table 3.

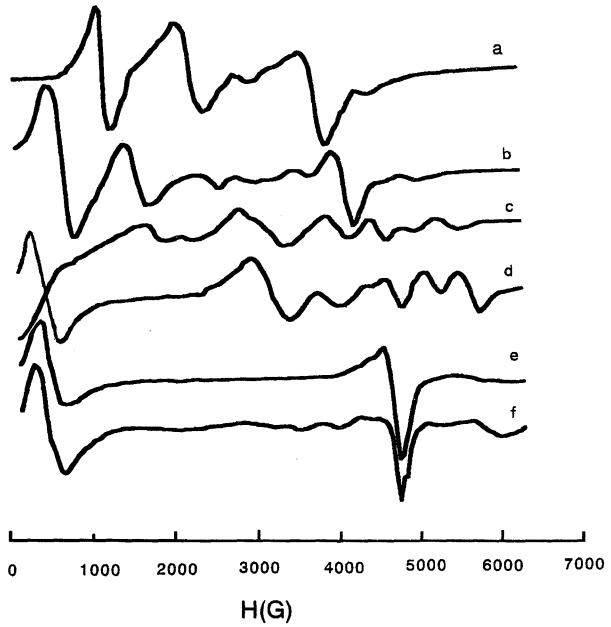

Fig. 2. Room temperature polycrystalline ESR spectra of $[Cu_2(O_2CCCl_3)_4(L)_2]\cdot nS$ at X-band frequency: curve a, L=2-Et-py (17); curve b, L=Caf(3) (12); curve c, L=2, 5-Cl_2-py (9); curve d, L=3-Cl-py (8); curve e, L=2-Cl-py (6); curve f, L=2-F-benzothiazol (1). The numbers in the parentheses designate the complexes listed in Table 1.

Table 3. Electronic Reflectance Spectral Data with Singlet–Triplet Separations for $[Cu_2(O_2CCCl_3)_4(L)_2]\cdot nS$

Compound[a]	$\bar{\nu}_{max} \times 10^{-3}$		$\Delta\bar{\nu}_{max} \times 10^{-3}$ [b]	$-2J$[c]
	cm^{-1}		cm^{-1}	cm^{-1}
1	12.58	7.81	4.77	240
2	12.50	7.46	5.04	237
3	12.90	7.69	5.21	229
4	12.20	8.33	3.87	224
5	12.58	8.00	4.58	220
6	12.70	7.80	4.90	220
7	12.39	7.79	4.60	195
8	12.50	7.57	4.93	193
9	12.98	9.09	3.89	191
10	11.76	9.35	2.41	141
11	12.82	10.86	1.96	138
12	12.05	10.00	2.05	136
13	12.66	10.41	2.25	131
14	12.50	10.52	1.98	107
15	11.63	9.52	2.11	102
16	12.19	10.10	2.09	95
17	13.33	11.63	1.70	79
2-Me-py	12.82	7.69	5.13	234
2-F-py	12.82	7.69	5.13	225
2,4-Me_2-py	12.66	7.69	4.97	223
2-Br-py	12.63	7.58	5.05	217
2,3-Me_2-py	11.36	7.52	3.84	215
3-Br-py	12.50	7.57	4.93	191
py	12.27	8.40	3.89	188
py·0.5C_6H_6	12.34	10.31	2.03	139
2,5-Me_2-py	12.34	9.80	2.54	136
2,4-Me_2-py·C_6H_6	12.66	10.53	2.13	99
3,5-Cl_2-py	13.51	11.62	1.89	92
4-Me-py·C_6H_6	12.34	10.31	2.03	86
3-Me-py	14.28	12.50	1.78	83
3,5-Me_2-py	12.99	11.23	1.76	74

a) See the footnote in Table 1 for the designation of the compounds, nos. 1—17; for the others, the name of the monodentate non-carboxylato ligand (L) is given along with the solvent molecule (S).[9,14,19] b) The separation between the two peaks. c) Singlet–triplet separation: see Table 1, footnote b.

Table 4. IR Spectral and Structural Data for $[Cu_2(O_2CCCl_3)_4(L)_2]\cdot nS$[a]

Compound[a]	$\bar{\nu}_{asym}$[b]	$\bar{\nu}_{sym}$[c]	$\Delta\bar{\nu}$[d]	Band width[e]	Cu–O (long)[f]
	cm^{-1}	cm^{-1}	cm^{-1}	cm^{-1}	Å
1	1691	1370	321	37	1.979[g]
2	1694	1371	323	38	1.981[g]
3	1691	1379	312	59	1.987[g]
4	1689	1370_{sh}	319	38	1.972[h]
5	1690	1374	316	—	1.968[g]
6	1691	1379	312	43	1.973[i]
7	1694	1368	326	—	1.987[j]
8	1692	1380	312	57	1.981[g]
9	1693	1362	331	42	2.130[g]
10	1695	1358	337	—	2.252[g]
11	1698	1345_{sh}	353	68	2.264[g]
12	1696	1364_{sh}	332	—	2.167[g]
13	1698	1360	338	33	2.21[g]
14	1698_{sh}	1342	356	68	2.237[g]
15	1701	1350	351	53	2.248[g]
16	1700	1340_{sh}	360	—	2.226[g]
17	1705	1345	360	61	2.328[g]

a) For the numbering of the compounds, see the footnote of Table 1. b) Antisymmetric COO^- stretching frequency. c) Symmetric COO^- stretching frequency. d) The difference between $\bar{\nu}_{asym}$ and $\bar{\nu}_{sym}$. e) Band width of antisymmetric COO^- stretching band at 1/2 height. f) The longest Cu–O bond.[14] g) Ref. 14. h) Ref. 15. i) Ref. 18. j) Ref. 17.

conclusion concerning the axial symmetry.

On the basis of the g-value criterion, as described above, and the characteristics of the electronic spectra, given in the subsequent section, a $d_{x^2-y^2}$ ground state is suggested to be present in the TCAC complexes, although an admixture of the d_{z^2} with the $d_{x^2-y^2}$ orbital in the ground state should be present, depending on the extent of the distortion from SP toward the TBP metal geometry. In the above study, the metal geometry of TCAC is thus described as SP or SP distorted toward TBP (SPDTBP) in which the longest Cu–O

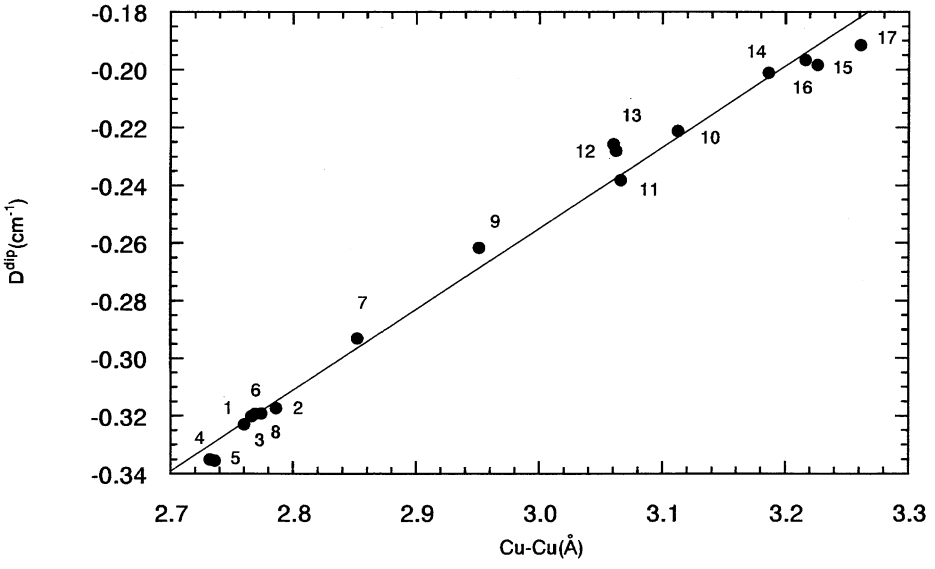

Fig. 3. D^{dip} vs. Cu···Cu distance for $[Cu_2(O_2CCCl_3)_4(L)_2]\cdot nS$.

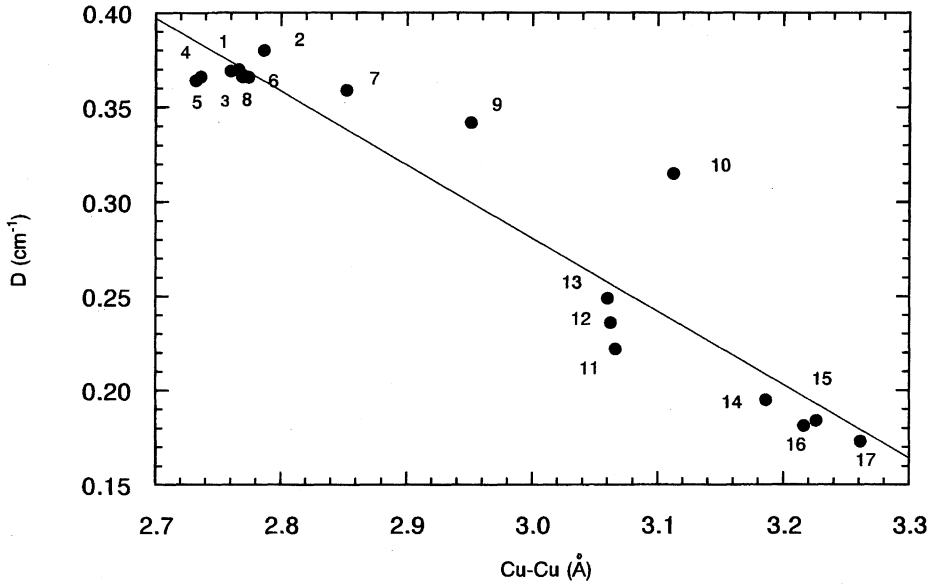

Fig. 4. D vs. Cu···Cu distance for $[Cu_2(O_2CCCl_3)_4(L)_2]\cdot nS$.

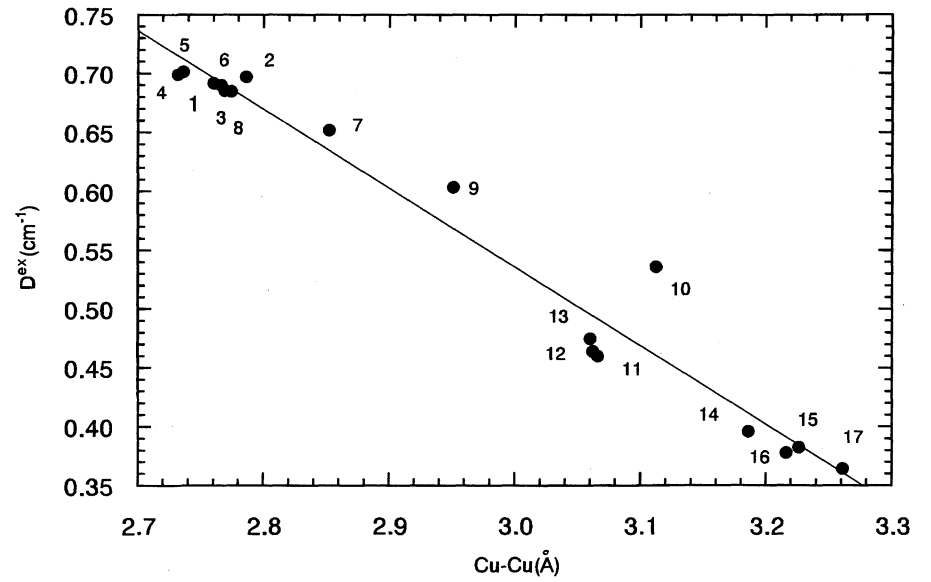

Fig. 5. D^{ex} vs. Cu···Cu distance for $[Cu_2(O_2CCCl_3)_4(L)_2]\cdot nS$.

bond is the main axis.[34]

The distortion of the metal geometry about copper, resulting in an increase in the Cu···Cu distance in TCAC, can be depicted in two ways: distorted square pyramidal with the main axis along the longest Cu–O bond and distorted trigonal bipyramidal with the axis along two successive Cu–O bonds, O–Cu–O. Which geometrical description is more appropriate depends upon the extent of the distortion from SP toward TBP. In the preceding paper,[14] we chose the latter. However, the present ESR and electronic spectral studies on TCAC, in which the longest Cu–O bond is 2.328 Å, suggests that the former standpoint is likely to be more appropiate. A schematic representation of the orbital overlaps of the exchange pathway in TCAC is given from the former viewpoint in Fig. 6. The overlap between the symmetric

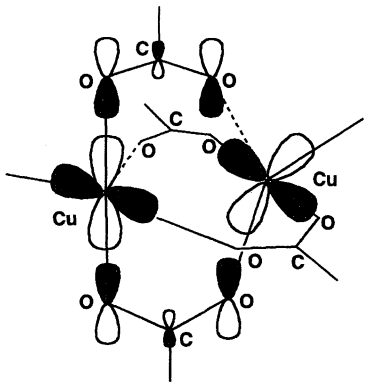

Fig. 6. Schematic representation of the orbital overlaps in the exchange pathway in $[Cu_2(O_2CCCl_3)_4(L)_2]\cdot nS$. The dashed lines represent the longest Cu–O bonds.

highest occupied MO's (HOMO's) of the bridging trichloroacetate ions and the essentially symmetric copper MO, which consists of $d_{x^2-y^2}$ orbitals, is considerably smaller at the longest Cu–O bonds. Thus, the $-2J$ value of TCAC is reduced along with a lengthening of the Cu–O bond based on the above viewdpoint.[3,10,22,35,36] It is noted that there exists a good correlation with a positive slope between the longest Cu–O bonds and the Cu···Cu distances (see Tables 2 and 4).

Electronic Spectra. The reflectance spectral data for compounds 1—17 are given in Table 3 along with fourteen additional compounds for which the $-2J$ values have been determined, but the structural data have not been reported. In Fig. 7, selected reflectance spectra of TCAC complexes whose geometry varies from SP toward TBP (SPDTBP) are given. Generally, (acetato)copper(II) adducts show two absorptions in the visible region: a high-energy absorption and a low-energy shoulder.[9] The TCAC with SP coordination geometry show the same type of spectra as the (acetato)copper(II) adducts, although the high-energy absorption is slightly shifted toward the low-energy side. It is known that, irrespective of monomeric or polymeric copper(II) complexes, when the distortion of the copper geometry from SP toward TBP increases, the intensity of the shoulder on the low-energy side increases and the separation of the two peaks, $\Delta\bar{\nu}_{max}$, decreases.[9,37] When a considerable distortion of the geometry occurs, the intensities of the two absorptions become approximately the same (twin-peaked spectrum), as shown in Fig. 7, curves d, e and f.[9,38—40] The correlation between the Cu···Cu distance and $\Delta\bar{\nu}_{max}$ is shown in Fig. 8. In order to examine the correlation of $\Delta\bar{\nu}_{max}$ with $-2J$,[41] linear-regression analyses were carried out on the three groups of complexes listed in Table 3: the unnumbered, the numbered, and all of the complexes. The three analyses give similar results (see Table 2), suggesting that the unnumbered complexes for which structural data are not available, should have essentially the same magneto-structural trend as the numbered complexes.

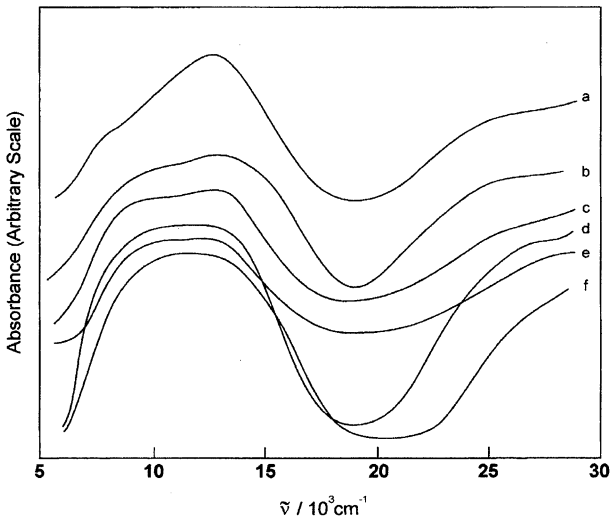

Fig. 7. Reflectance spectra of $[Cu_2(O_2CCCl_3)_4(L)_2]\cdot n$S: a, L=2-F-benzothiazol (1); b, L=1/2Caffeine, nS=2Toluene (5); c, L=2,5-Cl_2-py (9); d, L=2,5-Cl_2-py, ns=Benzene (10); e, L=2-Cl-5-NO_2-py (13); f, L=2-Et-py (17). The numbers in the parentheses designate the complexes listed in Table 3.

In order to obtain information about the metal ground state on the basis of the relationship of similar electronic spectra-similar ligand fields and metal geometries,[37] a comparison has been made between the O–Cu–O bond angles (the main axes assuming TBP metal geometry) and the corresponding bond angles for the reported copper(II) complexes having similar twin-peaked spectra. The N–Cu–N bond angle for $[CuCl(bpy)_2]NO_3\cdot 3H_2O$[38] is 174.9° with a peak separation of 2×10^3 cm^{-1}, the N–Cu–N bond angle for $[Cu(NCS)(bpy)_2]BF_4$[39] is 174.7° with a peak separation of 2.95×10^3 cm^{-1}, and the N–Cu–N bond angle for $[Cu(CN)(bpy)_2]NO_3\cdot 2H_2O$[40] is 170.9° with a peak separation of 2.1×10^3 cm^{-1}. A comparison of the bond angles and peak separa-

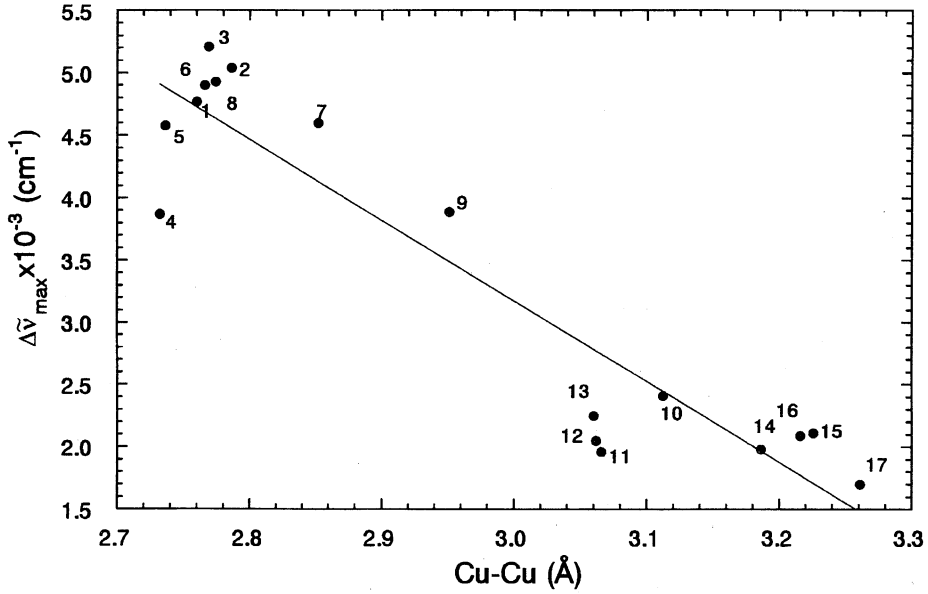

Fig. 8. $\Delta\bar{\nu}_{max}$ vs. Cu···Cu distance for $[Cu_2(O_2CCCl_3)_4(L)_2]\cdot n$S.

tions of these three complexes having SPDTBP structures (with which a $d_{x^2-y^2}$ ground state is assumed) with the corresponding parameters for $[Cu_2(O_2CCCl_3)_4(2\text{-Et-py})_2]$ (the two O–Cu–O bond angles=173.4° and 174.1°; the peak separation=1.7×10^3 cm^{-1}) suggests that these copper(II) complexes with those similar values of the O–Cu–O bond angle and $\Delta\overline{\nu}_{max}$ should have essentially the same metal geometry and the ground state, $d_{x^2-y^2}$, irrespective of the different coordinating atoms in the complexes.

Infrared Spectra. The infrared spectral data are listed along with the longest Cu–O bond distances[14] in Table 4. A good linear correlation with a positive slope has been found between the $\Delta\overline{\nu}$ ($=\overline{\nu}_{asym}-\overline{\nu}_{sym}$) values for the carboxylato ligands and the Cu···Cu distances (see Fig. 9 and Table 2). A similar correlation with a positive slope has been observed between $\overline{\nu}_{asym}$ and the Cu···Cu distances. Other linear correlations, such as $\Delta\overline{\nu}$ or $\overline{\nu}_{asym}$ vs. the longest Cu–O bond distances in the complexes, are also observed (see Table 2). The $\Delta\overline{\nu}$ value is related to the symmetry of the carboxylato ligands: the greater is the deviation from C_{2v} symmetry, the larger are the $\Delta\overline{\nu}$ values.[42—44] The linear correlation between the $\Delta\overline{\nu}$ values and the Cu···Cu distances clearly indicates that the deformation of the cage structure from SP toward TBP is related to a departure of the carboxylato ligand from C_{2v} symmetry. As the geometry of the copper(II) coordination sphere changes from SP toward TBP, the Cu–O bond distances in the cage structure vary over a considerable range in such a way that an alternate elongation and shortening of the Cu–O bonds to a bridging carboxylato ligand occurs.[14] This elongation and shortening of the Cu–O bond leads to a departure of the bridging carboxylato ligands from C_{2v} symmetry in that a long (weak) Cu–O bond is combined with a short (strong) C–O bond and a short (strong) Cu–O bond with a long (weak) C–O bond. Such a relationship between the strength of the coordinating bond and the asymmetry of carboxylato ligand has been observed by Nakamoto

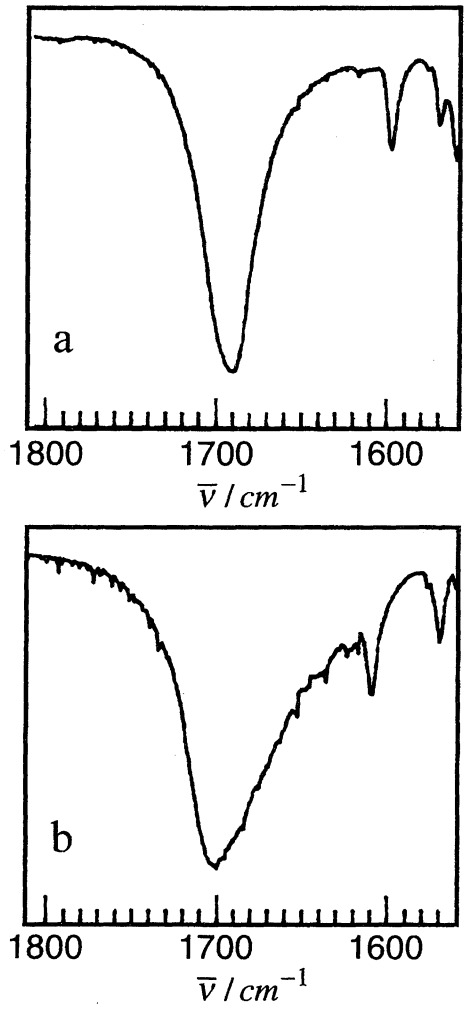

Fig. 10. Antisymmetric stretching absorption curves of two representative complexes, a [(1) SP; $-2J=240$ cm^{-1}] and b [(17) SPDTBP; $-2J=79$ cm^{-1}]. The numbers in the parentheses designate the complexes listed in Table 4.

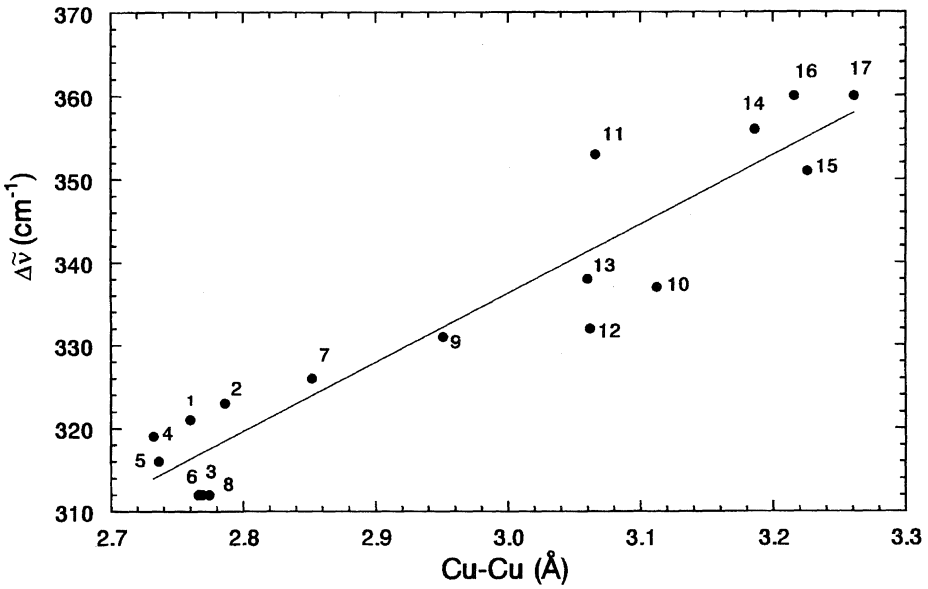

Fig. 9. $\Delta\overline{\nu}$ vs. Cu···Cu distance for $[Cu_2(O_2CCCl_3)_4(L)_2]\cdot nS$.

et al.[42,45,46] An infrared spectroscopic study on metal complexes of amino acids shows that a stronger metal–oxygen interaction results in a more asymmetric carboxylato ligand and an increase in $\overline{\nu}_{asym}$. Thus, the departure of the carboxylato ligand from C_{2v} symmetry produces an increase in both $\Delta\overline{\nu}$ and $\overline{\nu}_{asym}$. Furthermore, band broadening and/or splitting in the COO^- symmetric and asymmetric stretching regions occurs as a result of the low symmetry of the cage structure of the TCAC with a SPDTBP coordination sphere. Also, as the cage is distorted from SP toward TBP, the asymmetric COO^- stretching frequency increases along with the absorption band width at 1/2 height. The band width of the asymmetric COO^- stretching absorption can be used qualitatively as a guide to the geometry of the copper(II) coordination sphere and the carboxylato ligands in the cage. Typical examples of the asymmetric COO^- stretching absorption bands for two compounds (1 (SP) and 17 (SPDTBP)) are shown in Fig. 10.

The authors wish to express their thanks to Professor Dante Gatteschi of University of Florence for his helpful discussions.

References

1) R. W. Jotham, S. F. A. Kettle, and J. A. Marks, *J. Chem. Soc., Dalton Trans.*, **1972**, 428.

2) R. J. Doedens, "Progress in Inorganic Chemistry," ed by S. J. Lippard, John Wiley & Sons, New York (1976), Vol. 21, p. 209.

3) P. J. Hay, J. C. Thibeault, and R. Hoffmann, *J. Am. Chem. Soc.*, **97**, 4884 (1975).

4) J. Catterick and P. Thornton, *Adv. Inorg. Chem. Radiochem.*, **20**, 291 (1977).

5) P. de Loth, P. Cassoux, J. P. Daudey, and J. P. Malrieu, *J. Am. Chem. Soc.*, **103**, 4007 (1981).

6) M. Melnik, *Coord. Chem. Rev.*, **36**, 1 (1981).

7) M. Melnik, *Coord. Chem. Rev.*, **42**, 259 (1982).

8) D. N. Hendrickson, "Magneto-Structural Correlations in Exchange Coupled Systems," ed by R. D. Willett, D. Gatteschi, and O. Kahn, D. Reidel, Dordrecht (1984), NATO ASI Ser. C, Vol. 140, p. 523.

9) M. Kato and Y. Muto, *Coord. Chem. Rev.*, **92**, 45 (1988).

10) M. Yamanaka, H. Uekusa, S. Ohba, Y. Saito, S. Iwata, M. Kato, T. Tokii, Y. Muto, and O. W. Steward, *Acta Crystallogr., Sect. B*, **B47**, 344 (1991).

11) S. Ohba, M. Kato, T. Tokii, Y. Muto, and O. W. Steward, *Mol. Cryst. Liq. Cryst.*, **233**, 335 (1993).

12) A. Harada, M. Tsuchimoto, S. Ohba, K. Iwasawa, and T. Tokii, submitted for publication in *Acta Crystallogr., Sect. B.*

13) a) O. W. Steward, M. Kato, S.-C. Chang, M. Sax, C.-H. Chang, C. F. Jury, Y. Muto, T. Tokii, T. Taura, J. F. Pletcher, and C. S. Yoo, *Bull. Chem. Soc. Jpn.*, **64**, 3046 (1991); b) O. W. Steward, B. S. Johnston, S.-C. Chang, A. Harada, S. Ohba, T. Tokii, and M. Kato, *Bull. Chem. Soc. Jpn.*, **69**, 3123 (1996).

14) H. Uekusa, S. Ohba, T. Tokii, Y. Muto, M. Kato, S. Husebye, O. W. Steward, S.-C. Chang, J. P. Rose, J. F. Pletcher, and I. Suzuki, *Acta Crystallogr., Sect. B*, **B48**, 650 (1992).

15) M. Nakashima, M. Mikuriya, and Y. Muto, *Bull. Chem. Soc. Jpn.*, **58**, 968 (1985).

16) Y. Muto, M. Nakashima, T. Tokii, M. Kato, and I. Suzuki, *Bull. Chem. Soc. Jpn.*, **60**, 2849 (1987).

17) H. Horie, S. Husebye, M. Kato, E. A. Meyers, Y. Muto, I. Suzuki, T. Tokii, and R. A. Zingaro, *Acta Chem. Scand., Ser. A*, **40**, 579 (1986).

18) J. A. Moreland and R. J. Doedens, *Inorg. Chem.*, **17**, 674 (1978).

19) H. Horie, M. Nakashima, T. Tokii, Y. Muto, M. Kato, and I. Suzuki, "34th Symposium on Coordination Chemistry," Nagaoka, Japan, October 1984, Abstr., p. 476.

20) M.-L. Boillot, Y. Journaux, A. Bencini, D. Gatteschi, and O. Kahn, *Inorg. Chem.*, **24**, 263 (1985).

21) The values of the magnetic fields of the resonance used in obtaining the ESR parameters are deposited with the values of the parameters as Document No. 70020 at the Office of the Editor of Bull. Chem. Soc. Jpn.

22) P. K. Ross, M. D. Allendorf, and E. I. Solomon, *J. Am. Chem. Soc.*, **111**, 4009 (1989).

23) J. H. Price, J. R. Pilbrow, K. S. Murray, and T. D. Smith, *J. Chem. Soc. A*, **1970**, 968.

24) T. D. Smith and J. R. Pilbrow, *Coord. Chem. Rev.*, **13**, 173 (1974).

25) J. R. Pilbrow, "Transition Ion Electron Paramagnetic Resonance," Clarendon Press, Oxford (1990), Chap. 7, pp. 332—367.

26) Y. Muto, N. Hirashima, T. Tokii, M. Kato, and I. Suzuki, *Bull. Chem. Soc. Jpn.*, **59**, 3672 (1986).

27) J. R. Wasson, C-I. Shyr, and C. Trapp, *Inorg. Chem.*, **7**, 469 (1968).

28) M. Nakashima, T. Tokii, Y. Muto, S. Ohba, O. W. Steward, M. Kato, and I. Suzuki, "30th International Conference on Coordination Chemistry," Kyoto, July 1994, Abstr., PS2-52, p. 182.

29) A detailed discussion on the relationship between the $-2J$ and D in MPAC and TCAC will be made in a subsequent paper.

30) B. J. Hathaway and D. E. Billing, *Coord. Chem. Rev.*, **5**, 143 (1970).

31) M. Suzuki, H. Kanatomi, H. Koyama, and I. Murase, *Bull. Chem. Soc. Jpn.*, **53**, 1961 (1980).

32) T. R. Felthouse, E. J. Laskowski, and D. N. Hendrickson, *Inorg. Chem.*, **16**, 1077 (1977).

33) L. P. Battaglia, A. B. Corradi, G. Marcotrigiano, L. Menabue, and G. C. Pellacani, *Inorg. Chem.*, **20**, 1075 (1981).

34) S. Ohba, *Nippon Kessho Gakkai Shi*, **35**, 334 (1993).

35) O. Kahn, "Magneto-Structural Correlations in Exchange Coupled Systems," ed by R. D. Willett, D. Gatteschi, and O. Kahn, D. Reidel, Dordrecht (1985), NATO ASI Ser. C, Vol. 140, pp. 37—85; O. Kahn, "Structure and Bonding," Springer-Verlag, Berlin (1987), Vol. 68, pp. 89—167; O. Kahn, "Molecular Magnetism," VCH Pub. Inc., New York (1993), pp. 145—183.

36) A. Bencini and D. Gatteschi, "Electron Paramagnetic Resonance of Exchange Coupled Systems," Springer-Verlag, Berlin (1990), pp. 1—19.

37) N. Ray, L. Hulett, R. Sheahan, and B. J. Hathaway, *Inorg. Nucl. Chem. Lett.*, **14**, 305 (1978).

38) W. D. Harrison, D. M. Kennedy, M. Power, R. Sheahan, and B. J. Hathaway, *J. Chem. Soc., Dalton Trans.*, **1981**, 1556.

39) S. Tyagi and B. J. Hathaway, *J. Chem. Soc., Dalton Trans.*, **1981**, 2029.

40) S. Tyagi and B. J. Hathaway, *J. Chem. Soc., Dalton Trans.*, **1983**, 199.

41) There is a good linear correlation between the $-2J$ values and the Cu···Cu distances for the numbered compounds in Table 2.[14] Accordingly, the $-2J$ values can be used in place of the Cu···Cu distances.

42) K. Nakamoto, "Infrared and Raman Spectra of Inorganic and Coordination Compounds," 4th ed, John Wiley & Sons, New York (1986), pp. 231—233.
43) R. C. Mehrotra and R. Bohra, "Metal Carboxylates," Academic Press, London (1983), pp. 48—60.
44) S. Emori, K. Ohishi, H. Kurihara, and Y. Muto, *Bull. Chem. Soc. Jpn.*, **61**, 4439 (1988).
45) K. Nakamoto, Y. Morimoto, and A. E. Martell, *J. Am. Chem. Soc.*, **83**, 4528 (1961).
46) K. Nakamoto, Ref. 40, p. 233.